

miR156-Targeted and Nontargeted SBP-Box Transcription Factors Act in Concert to Secure Male Fertility in *Arabidopsis*

Shuping Xing,^{a,1} María Salinas,^{a,b} Susanne Höhmann,^a Rita Berndtgen,^a and Peter Huijser^a

^aDepartment of Molecular Plant Genetics, Max Planck Institute for Plant Breeding Research, 50829 Cologne, Germany

^bÁrea de Genética, Departamento de Biología Aplicada, Universidad de Almería, 04120 Almería, Spain

The SBP-box transcription factor *SQUAMOSA PROMOTER BINDING PROTEIN-LIKE8* (*SPL8*) is required for proper development of sporogenic tissues in *Arabidopsis thaliana*. Here, we show that the semisterile phenotype of *SPL8* loss-of-function mutants is due to partial functional redundancy with several other members of the *Arabidopsis SPL* gene family. In contrast with *SPL8*, the transcripts of these latter *SPL* genes are all targeted by miR156/7. Whereas the introduction of single miR156/7-resistant *SPL* transgenes could only partially restore *spl8* mutant fertility, constitutive overexpression of miR156 in an *spl8* mutant background resulted in fully sterile plants. Histological analysis of the anthers of such sterile plants revealed an almost complete absence of sporogenous and anther wall tissue differentiation, a phenotype similar to that reported for *sporocyteless/nozzle* (*spl/nzz*) mutant anthers. Expression studies indicated a functional requirement for miR156/7-targeted *SPL* genes limited to early anther development. Accordingly, several miR156/7-encoding loci were found expressed in anther tissues at later stages of development. We conclude that fully fertile *Arabidopsis* flowers require the action of multiple miR156/7-targeted *SPL* genes in concert with *SPL8*. Either together with *SPL/NZZ* or independently, these *SPL* genes act to regulate genes mediating cell division, differentiation, and specification early in anther development. Furthermore, *SPL8* in particular may be required to secure fertility of the very first flowers when floral transition-related miR156/7 levels might not have sufficiently declined.

INTRODUCTION

Flowering plants alternate during their life cycle between diploid sporophytic and haploid gametophytic generations. Initial development of the sporophyte arising from the zygote is generally dominated by vegetative growth. Sexual reproduction requires a developmental phase transition resulting in the formation of flowers with highly specialized organs (i.e., anther-bearing stamens and ovule-bearing carpels). Within these organs, cells are recruited to undergo meiotic divisions to form male and female gametophytes. In *Arabidopsis thaliana*, the canonical homeotic ABC genes *APETALA3*, *PISTILLATA*, and *AGAMOUS* (*AG*) determine stamen identity of the third whorl floral organs. The latter is a direct activator of *SPOROCTELESS/NOZZLE* (*SPL/NZZ*) more recently found to play a role in determining stamen identity also (Ito et al., 2004; Liu et al., 2009). After stamen identity is fixed, subsequent anther development can be divided into 14 stages according to defined histological characteristics (Sanders et al.,

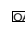
1999). Stages 1 to 7 are predominantly confined to sporogenous cell and anther wall formation in the four corners of the anther. The postmeiotic stages 8 to 14 mainly consist of pollen maturation and anther structural adaptations for their release at anthesis.

Much research on early anther development has focused on how sporogenous and parietal cells are derived and how they interact in a complex process involving cell proliferation, specification, and differentiation. However, whereas comparative global expression analysis of the wild type and mutants uncovered many genes acting specifically in early anther development (Zik and Irish, 2003; Hennig et al., 2004; Wellmer et al., 2004; Lu et al., 2006; Alves-Ferreira et al., 2007; Ma et al., 2007, 2008; Wijeratne et al., 2007), only a few are functionally characterized. Among the earliest acting genes are those that relate to more general aspects of organ growth like regulating polarity and cell proliferation, such as the related transcription factors *JAGGED* and *NUBBIN* (Dinneny et al., 2006; reviewed in Husbands et al., 2009). Their activity is followed by the determination of cell fate within anthers, but little is known about genes that participate in the specification of the archesporial cells. However, obviously required for early microsporangium development are *SPL/NZZ* and *ROXY1* and -2, as their respective mutants do not produce microsporocytes and anther walls (Schieffhale et al., 1999; Yang et al., 1999; Xing and Zachgo, 2008). Subsequent cell-type specification and differentiation is mediated by *BARELY ANY MERISTEM1* (*BAM1*) and *BAM2*, *EXCESS MICROSPOROCTES1/EXTRA SPOROGENOUS*

¹ Address correspondence to xing@mpiz-koeln.mpg.de.

The authors responsible for distribution of materials integral to the findings presented in this article in accordance with the policy described in the Instructions for Authors (www.plantcell.org) are: Shuping Xing (xing@mpiz-koeln.mpg.de) and Peter Huijser (huijser@mpiz-koeln.mpg.de).

 Online version contains Web-only data.

 Open Access articles can be viewed online without a subscription. www.plantcell.org/cgi/doi/10.1105/tpc.110.079343

CELLS (*EMS1/EXS*), SOMATIC EMBRYOGENESIS RECEPTOR-LIKE KINASE1 (*SERK1*) and *SERK2*, and TAPETUM DETERMINANT1 (*TPD1*) (Canales et al., 2002; Zhao et al., 2002; Yang et al., 2003; Albrecht et al., 2005; Colcombet et al., 2005; Hord et al., 2006; Mizuno et al., 2007; Jia et al., 2008; Zhao, 2009). Their mutants all produce more micromeiocytes at the expense of tapetum or other parietal cell layers due to ectopic expression of *SPL/NZZ*. In normal development, *SPL/NZZ* promotes expression of *BAM1* and *BAM2* such that in a negative feedback, *BAM1* and *BAM2* restricts *SPL/NZZ* to the center of the locule (Hord et al., 2006). Whereas *BAM1*, *BAM2*, *EMS1/EXS*, *SERK1*, *SERK2*, and *TPD1* all encode receptor/ligand components, *SPL/NZZ* remains the only transcription factor studied in detail at these early anther stages (Ma, 2005).

In previous work, we showed that in addition to *SPL/NZZ*, the unrelated SBP-box transcription factor *SPL8* influences anther development in *Arabidopsis* (Cardon et al., 1999; Unte et al., 2003; Zhang et al., 2007). Histological analysis of *spl8* loss-of-function mutants revealed abnormal pollen sac formation, resulting in reduced pollen production per anther and, as a consequence, a reduced fertility. Moreover, severity of the phenotype declined acropetally in the main inflorescence.

SBP-box genes, known in *Arabidopsis* as SBP-Like (*SPL*) genes, encode a plant-specific family of transcription factors binding DNA through the conserved SBP domain (Klein et al., 1996; Yamasaki et al., 2004; Birkenbihl et al., 2005). In recent years, members of this family in different plant species have functionally been linked to diverse developmental processes, such as seed germination and seedling development (Martin et al., 2010), leaf and plastocron development (Moreno et al., 1997; Wang et al., 2008), trichome formation and distribution (Yu et al., 2010), juvenile-to-adult and floral phase transitions (Cardon et al., 1997; Wu and Poethig 2006; Gandikota et al., 2007; Schwarz et al., 2008; Shikata et al., 2009; Wang et al., 2009; Wu et al., 2009), fruit ripening (Manning et al., 2006), as well as to copper homeostasis (Kropat et al., 2005; Yamasaki et al., 2009), programmed cell death (Stone et al., 2005), domestication (Wang et al., 2005), and grain yield (Jiao et al., 2010; Miura et al., 2010). Importantly, many of these SBP-box genes are targeted by the microRNAs (miRNAs) 156 and 157 (Reinhart et al., 2002; Schwab et al., 2005), a developmentally highly relevant interaction (see references above) and already found in the moss *Physcomitrella patens* (Arazi et al., 2005; Riese et al., 2007). Most interestingly, floral transition in *Arabidopsis* correlates with a decline in the level of miR156 and an increase of its targets (Wang et al., 2009; Wu et al., 2009).

As loss-of-function of *SPL8* results in a semisterile phenotype that declines in severity in an acropetal fashion, we investigated if a compensatory mechanism could rely on functional redundancy with other *Arabidopsis* SBP-box genes. Here, we present data that miR156/7 targeted *SPL* genes together with the nontargeted *SPL8* are absolutely required for male fertility in *Arabidopsis*. Either together with or independently of *SPL/NZZ*, these SBP-box transcription factors promote sporogenous cell and parietal cell formation in early anthers.

RESULTS

Loss-of-Function of miR156/7-Targeted SBP-Box Genes Enhances the *spl8* Semisterile Phenotype

Based on similarities in both SBP domain sequence and genomic structure, the 17 *Arabidopsis* *SPL* genes are easily divided into two groups. The first group is represented by the more complexly organized genes *SPL1*, -7, -12, -14, and -16, which consist of 10 or more exons and encode proteins of over 800 residues. The second group represents the remaining 12 *SPL* genes, with two to four exons and coding for proteins of less than half the size of those within the first group (Figure 1A; Riese et al., 2008). Moreover, with the exception of *SPL8*, all members of the second group carry a miR156/7 response element and are thus subjected to posttranscriptional regulation by miR156/7 (Figure 1A). It should be noted, however, that *SPL8* and other members of this group share very limited sequence similarity outside the SBP domain. In fact, additional similarity could be detected only weakly in the N-terminal region of *SPL2*, -10, -11, -9, and -15 and possibly also of *SPL13*. This area upstream of the SBP domain encompasses a motif with unknown function previously described to be evolutionary conserved for orthologous *SPL8*-like proteins (Unte et al., 2003; Riese et al., 2007).

To test the possibility that other SBP-box genes contribute redundantly to sustain fertility in *spl8*, we first identified the triple mutants *spl8 spl9 spl15*, *spl8 spl2 spl9*, and *spl8 spl2 spl15* and the quadruple mutant *spl8 spl2 spl9 spl15* from an F2 population generated after a cross between *spl8-1* and the triple mutant *spl2-1 spl9-1 spl15-1* (Schwarz et al., 2008), a loss-of-function mutant for the *SPL2*, *SPL9*, and *SPL15* genes, which are posttranscriptionally regulated by miR156 and probably by miR157 as well (Figure 1A). When compared with the *spl8-1* single mutant, the identified multiple mutants were found to form, as expected, fewer pollen sacs and less pollen in the anthers of later arising flowers (Figures 1B and 1C). Hence, seed production of these plants dramatically decreased (Figure 1D). Pollen production and seed set in the triple mutant *spl2-1 spl9-1 spl15-1*, however, was only slightly reduced (Figures 1C and 1D). These data provided evidence that the miR156/7-targeted *SPL* genes do affect fertility. That they regulate anther development, most probably redundantly with *SPL8*, was therefore further investigated as described below.

Overexpression of *MIR156* in an *spl8* Mutant Background Leads to Full Male Sterility

The quadruple mutant *spl8 spl2 spl9 spl15* occasionally produced a few seeds per silique (Figure 1D). To examine whether this leakiness is due to other still functioning miR156/7-mediated SBP-box genes in the *spl8* mutant, we crossed *spl8-1* into a homozygous *35S:MIR156b* transgenic line in which the targeted *SPL* genes were confirmed to be all downregulated (Schwab et al., 2005; see Supplemental Figure 1 online). In their reproductive phase, these miR156-overexpressing plants were bushy with short siliques (Figure 2A). In addition, pollen production per anther and seed set per silique of these plants were also reduced to ~15 and 50%, respectively, of that of the wild type (30 anthers

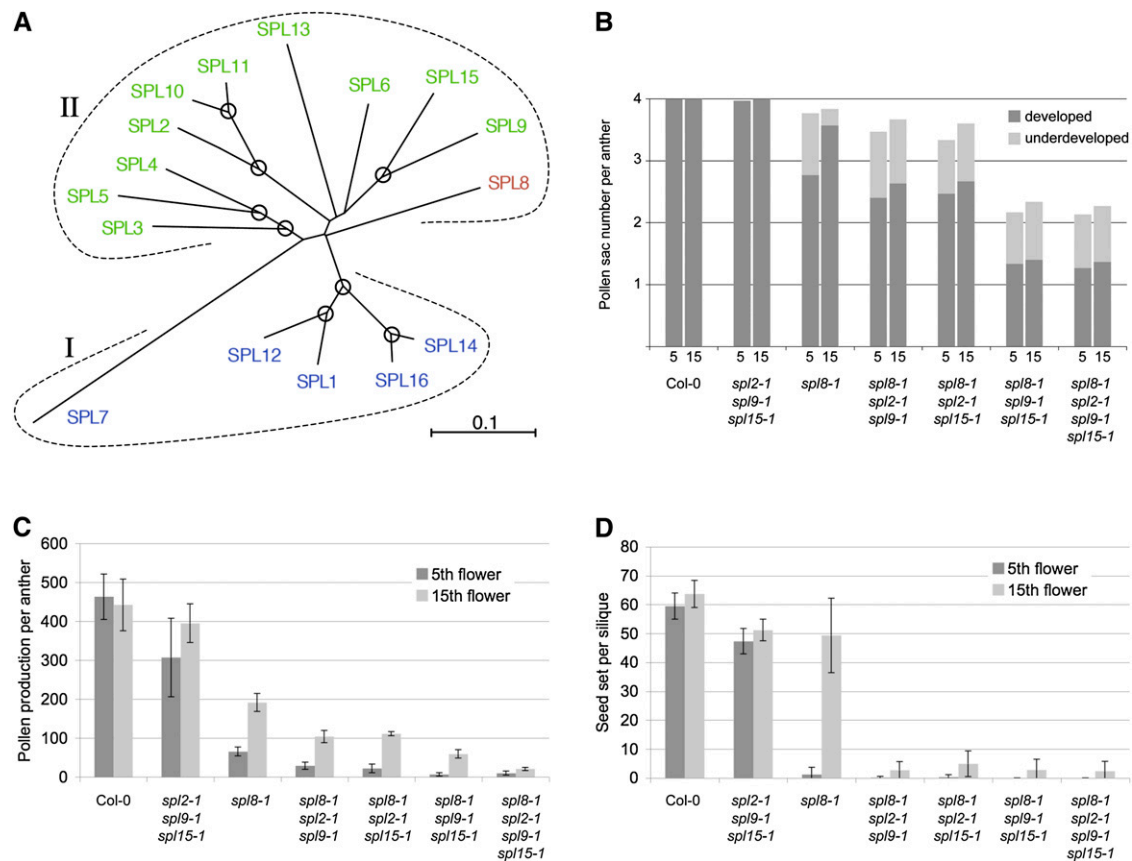


Figure 1. Phylogenetic Relationships among *SPL* Gene Family Members in *Arabidopsis* and Exposed Redundancy in Fertility.

(A) Unrooted phylogram of all *SPL* genes obtained using the neighbor-joining algorithm and based on the conserved SBP domain. Nodes representing bootstrap values >50% from 10,000 replicates are encircled. Both subfamilies I and II are indicated by dashed lines. *miR156/7*-targeted *SPL* genes are depicted in green, whereas nontargeted large *SPL* genes and *SPL8* are in blue and red, respectively. The alignment used to generate this tree is available as Supplemental Data Set 1 online.

(B) and **(C)** Mean number of pollen sacs **(B)** and mean number of pollen **(C)** formed per anther of the wild type and mutants for *SPL8*, *SPL2*, *SPL9*, and *SPL15* and combinations thereof, as labeled in the image. A total of 30 anthers from the 5th and 15th flowers of six primary inflorescences were analyzed. Small pollenless locules are referred to as underdeveloped.

(D) Mean number of seeds set per silique of the wild type and multiple *SPL* gene mutants as labeled in the image. Siliques from the 5th and 15th flowers of a total of 20 primary inflorescences were examined. Error bars indicate sd.

and 22 siliques examined, respectively). However, whereas the parental *spl8-1* and *35S:MIR156b* transgenic plants still produced some seeds, 29 out of 160 F₂ plants showed a fully sterile phenotype under comparable growth conditions (Figure 2A). All of these sterile plants were genotyped as homozygous for *spl8-1* with one or two copies of the *35S:MIR156b* transgene. Further geno- and phenotyping also revealed that a loss of *SPL8* function enhanced the short and bushy phenotype of both the hemi- and homozygous *35S:MIR156b* transgenics in a dosage-dependent manner. In addition, the flowers of the fully sterile double mutant plants produced trichomes on the adaxial instead of on the abaxial sides of their sepals (Figure 2D). In their overall size, the flowers did resemble those of the *35S:MIR156b* transgenic line in size (i.e., displaying a squashed appearance but anthers remained small and did not release pollen) (Figures 2B to 2D; Schwab et al., 2005). To examine the fertility of the female

organs of double mutant plants harboring one or two copies of the *35S:MIR156b* transgene, we manually pollinated the club-shaped and short-stalked pistils with wild-type pollen (Figure 2C, inset). Three weeks after pollination, siliques of such plants homozygous for *spl8-1* and hemizygous for the *35S:MIR156b* transgene had slightly elongated and contained four to eight seeds per silique (20 siliques examined). Siliques of plants homozygous for both *spl8-1* and the *35S:MIR156b* transgene carried only zero to three seeds per silique (21 siliques examined). Similar results were obtained with *35S:MIR156a spl8-2* and *35S:MIR156 h spl8-1* mutant plants (20 and 24 siliques examined, respectively). These results show that downregulation of *miR156*-targeted *SPL* genes in *spl8* mutants resulted in nearly fully sterile plants. The observed residual female fertility may reflect leakiness in the repression of the *miR156*-targeted *SPL* genes by the *35S:MIR156* transgene.

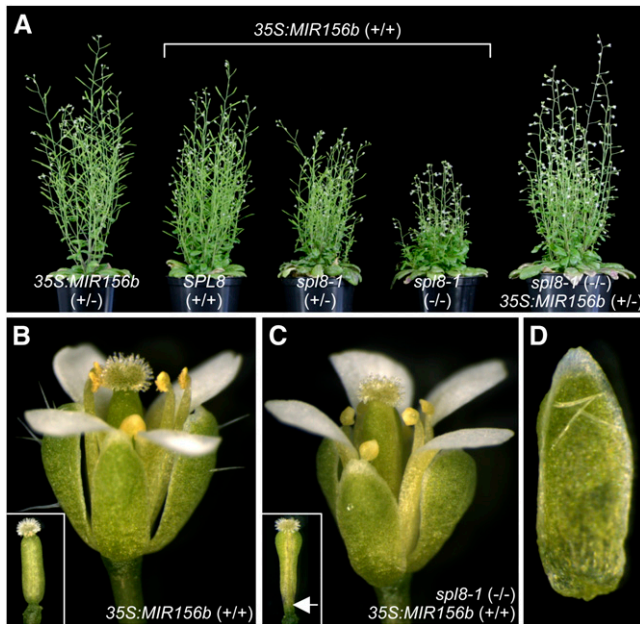


Figure 2. Reproductive Phenotypes of 35S:MIR156b *spl8-1* Plants.

(A) Morphology of 6-week-old 35S:MIR156b and 35S:MIR156b *spl8-1* plants under long-day growth conditions. Homo- or hemizyosity for the 35S:MIR156b transgene is indicated by (+/+) or (+/-), respectively, and homo- or heterozygosity for the *spl8-1* mutant allele respectively by (-/-) or (+/-).

(B) 35S:MIR156b (+/+) flower at anthesis showing dehiscent anthers releasing pollen to the stigma. Sepals carry trichomes on their abaxial side. Inset in the bottom left corner shows the pistil dissected from the same flower.

(C) Flower at anthesis from a plant homozygous for both the 35S:MIR156b transgene and the *spl8-1* mutant allele. The small anthers do not dehisce and are pollenless. Trichomes are largely absent from the abaxial side of the sepals. Inset in the bottom left corner shows the dissected pistil from the same flower with a swollen upper part and a short stalk (white arrow).

(D) A sepal from the flower shown in **(C)**, carrying adaxial trichomes.

miR156 Depletion by Sequestration Partially Rescues the *spl8* Semisterile Phenotype

So far, our results clearly showed that downregulation of miR156/7-targeted *SPL* genes strongly enhanced the *spl8* fertility problem. Usually, the first few flowers formed in the primary inflorescence of *spl8-1* mutants do not set seed at all. To investigate whether upregulation of miR156/7-targeted *SPL* genes could restore fertility in such flowers, we crossed a homozygous *spl8-1* mutant to a homozygous transgenic miR156 target mimicry line. These *MIM156* transgenic plants display a lengthened plastochron and flower after fewer leaves due to the upregulation of miR156-targeted *SPL* genes (Franco-Zorrilla et al., 2007). Furthermore, fertility of *MIM156* transgenic plants, as deduced from the seed set per silique, seemed only slightly reduced compared with the wild type (Figure 3C). In a resulting F2 population of 300 plants, we found 22 plants homozygous for *spl8-1* that carried at least one copy of the

MIM156 transgene. In comparison to the homozygous *spl8-1* mutant alone, these plants showed a significantly (*t* test, $P < 0.05$) increased seed set, in particular with respect to the first flowers, although wild-type levels were not reached (Figures 3A to 3C). This partial rescue through upregulation of miR156-targeted *SPL* genes (see Supplemental Figure 2 online) further support the hypothesis that at least some of the latter genes act redundantly with *SPL8* to maintain fertility.

miR156-Resistant Forms of Several miR156/7-Targeted *SPL* Genes Attenuate the *spl8* Semisterile Phenotype

Eleven of the 17 *SPL* genes are targeted by miR156/7 (Figure 1A). To get a better impression of which of these are able to restore the *spl8* semisterile phenotype, we selected *SPL3*, -2, -11, -9, -15, -6, and -13 and constructed miR156/7-resistant forms of

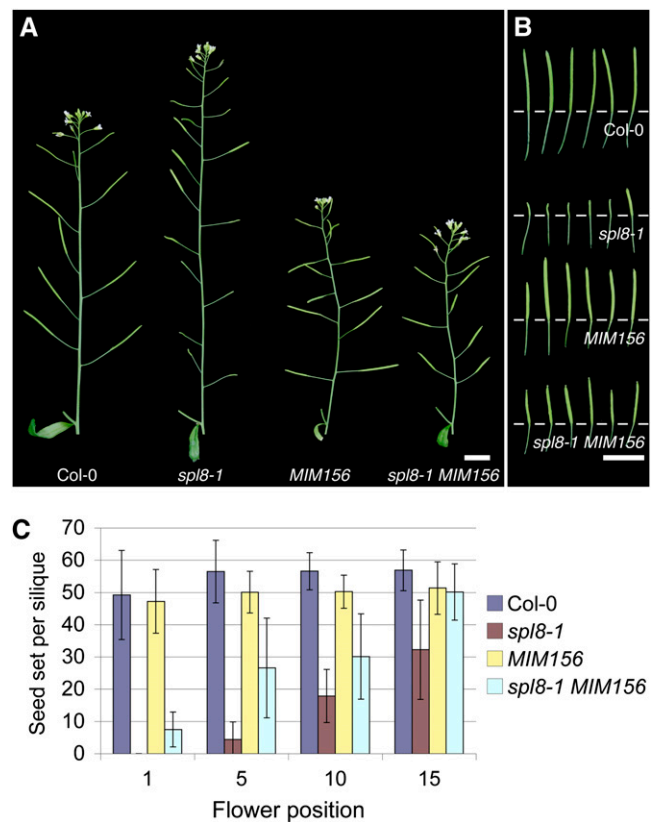


Figure 3. Effect of miR156 Target Mimicry on Seed Set in Wild-Type and *spl8-1* Mutant Plants.

(A) Primary inflorescences, cut off below the last cauline leaf, of wild-type and mutant plants as labeled in the image. Bar = 1 cm.

(B) Siliques from the 1st to 6th flower (left to right) formed within the primary inflorescences (arranged top to bottom as shown from left to right in **(A)**). Bar = 1 cm.

(C) Mean number of seeds set per silique from the 1st, 5th, 10th, and 15th flower, respectively, formed within the primary inflorescences of wild-type and mutant plants as labeled in the image. Error bars indicate SD ($n = 20$).

these genes (see Methods). Driven by a 2.1-kb upstream promoter region of the *SPL8* gene, these miR156/7-resistant versions, hereafter referred to as *rSPL3*, *rSPL2*, etc., were subsequently introduced into an *sp8-1* mutant background. As a control for full complementation, we transformed a similarly driven *SPL8* transgene into the *sp8-1* mutant. In the case of this control, 98% of all T1 plants displayed a wild-type-like fertility (i.e., full restoration of seed set; Table 1). By contrast, none of the T1 plants ($n = 300$) with *rSPL3* or *rSPL6* exhibited an improved fertility compared with *sp8-1*. For *rSPL2*, -9, -15, -11, and -13, only a low percentage (10 to 25%; $n = 80$ to 100) of the T1 plants displayed better fertility than *sp8-1*. To get a clue as to what might have caused only a minority of T1 plants to restore the *sp8* mutant fertility partially, we examined the expression of the *rSPL13* transgene in three partially rescued and three non-rescued transgenic plants selected randomly from a *pSPL8:rSPL13* T1 population. The results showed that all the partially rescued T1 plants expressed the transgene to higher levels than did the nonrescued plants (see Supplemental Figure 3 online).

To quantify the degree of fertility rescue, progeny of five partially rescued plants from each of the respective T1 populations were grown and their seed set per silique determined. The partially rescued *sp8* phenotype could still be observed in these T2 populations, although some segregation occurred, probably due to different transgene copy numbers. The seed set per silique is shown in Table 1.

Early Anther Development Is Affected in 35S:MIR156b *sp8-1* Plants

As described before, 35S:MIR156b *sp8-1* plants form small and fully sterile anthers. To investigate what aspects of anther histogenesis are affected in these plants, we prepared transverse semithin sections through anthers at different developmental stages for comparison to the wild type and the respective single mutants. In the wild type (Figures 4A to 4E), as reported previously, subepidermal archesporial cells became detectable in stage 2 anthers (Figure 4A; staging according to Sanders et al., 1999). At stage 3 (Figure 4B), their periclinal division gave rise to the primary parietal and sporogenous cells. Subsequent mitotic divisions of these cells and their progeny then resulted in the

distinct anther wall layers surrounding the pollen mother cells (PMCs) at stage 5 (Figure 4D). Meiotic divisions of the latter cells followed by microspore release from the tetrads, together with further differentiation of somatic anther tissues, eventually resulted in anther locules filled with mature pollen as seen in stage 12 (Figure 4E). In comparison, anther development in 35S:MIR156b transgenics seemed to follow the wild-type pattern, although less pollen was seen per locule (Figures 4F to 4J). By contrast, anther development in 35S:MIR156b *sp8-1* flowers deviated clearly (Figures 4P to 4T). Archesporial-like cells appeared and underwent a few mitotic divisions (Figures 4P and 4Q), similar to stages 2 and 3 in the wild type. However, there appeared to be fewer cells already in stage 3-like anther sections, probably due to reduced cell proliferation. In subsequent developmental stages, no typical sporogenous cells differentiated. One or two subepidermal cell layers could still be observed, but from these no distinct anther wall layers developed (Figure 4R). Instead, most of the anther cells became vacuolated (i.e., similar to the connective tissue in the wild type). A vascular strand developed, but formation of any pollen sacs failed (Figures 4S and 4T). This phenotype is much more severe than that of *sp8-1* single and of *sp8-1 sp2-1 sp9-1 sp15-1* quadruple mutants. In the anthers of these mutants, probably due to abnormal cell proliferation, the number and size of the final pollen sacs were reduced, but at least some pollen matured (Figures 4K to 4O; see Supplemental Figure 4 online).

To verify further that cell proliferation was affected in the 35S:MIR156b *sp8-1* anthers, we performed in situ hybridization using a *Histone H4* (*H4*) probe as a cycling cell marker. Comparison of wild-type and 35S:MIR156b *sp8-1* expression patterns at different anther developmental stages revealed that in anther stage 2, *H4* expression was already slightly reduced in 35S:MIR156b *sp8-1* (Figures 5A and 5E). This difference became more obvious at later stages. Whereas developing wild-type anthers kept highly active dividing cells, particular at their four corners, at least up until stage 5 (Figures 5B to 5D), expression of *H4* rapidly decreased in 35S:MIR156b *sp8-1* anthers (Figures 5F to 5H), indicative of fewer cell divisions. Taken together, these data demonstrate that *SPL8* together with miR156/7-targeted *SPL* genes are essential for proper cell proliferation in early anther development.

Table 1. Seed Set in Different Genotypes

Genotype	1st Flower			5th Flower			10th Flower			15th Flower		
	Mean	SD	<i>n</i>	Mean	SD	<i>n</i>	Mean	SD	<i>n</i>	Mean	SD	<i>n</i>
Col-0	59.5	5.8	20	63.4	6.6	22	68.3	5.1	22	65.8	4.3	22
<i>sp8-1</i>	0.0	0.0	21	2.3	3.4	21	39.3	15.0	23	53.8	6.6	24
<i>pSPL8:SPL8 sp8-1</i>	64.8	7.0	23	69.1	6.3	25	68.8	5.8	23	69.9	3.4	25
<i>pSPL8:rSPL3 sp8-1</i>	0.0	0.0	25	0.8	1.6	26	24.2	15.5	26	38.1	11.7	26
<i>pSPL8:rSPL6 sp8-1</i>	0.2	0.9	22	2.9	4.6	19	48.5	14.5	22	55.3	13.5	22
<i>pSPL8:rSPL2 sp8-1</i>	8.6	12.1	21	37.0	16.9	20	52.1	15.0	21	55.4	9.5	20
<i>pSPL8:rSPL9 sp8-1</i>	4.7	1.2	23	21.5	2.7	22	57.5	2.5	21	61.5	2.0	22
<i>pSPL8:rSPL15 sp8-1</i>	3.7	1.1	23	22.4	2.9	24	52.2	2.7	23	57.7	3.3	22
<i>pSPL8:rSPL11 sp8-1</i>	1.3	3.1	23	22.5	16.1	20	53.9	14.4	23	57.2	10.5	23
<i>pSPL8:rSPL13 sp8-1</i>	6.0	9.0	21	30.1	16.2	20	42.4	17.8	21	43.8	16.3	21

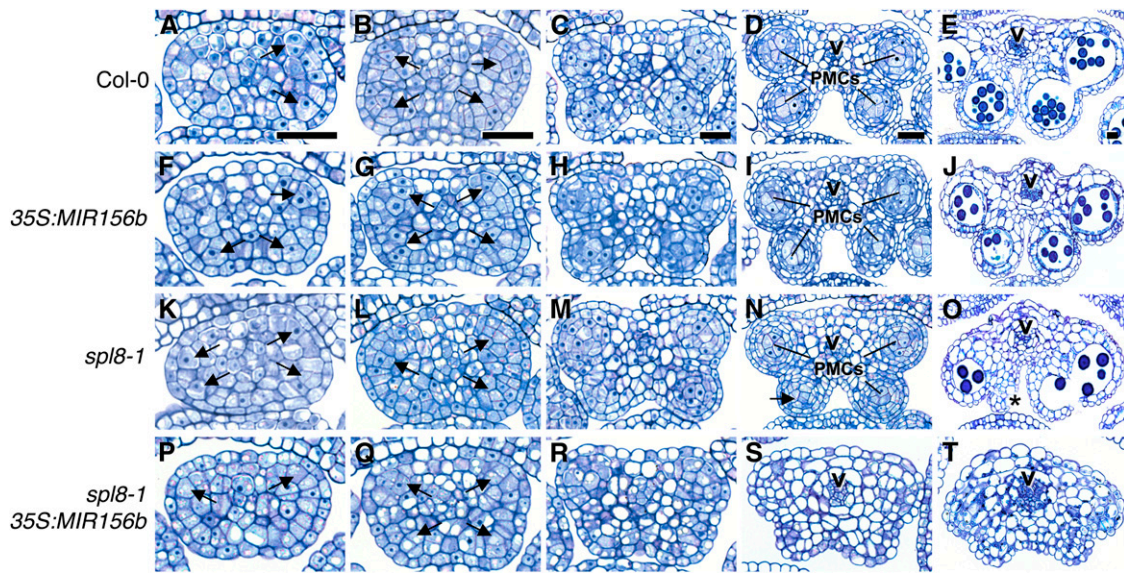


Figure 4. Comparative Histological Analysis of Anther Development.

(A) to (T) Toluidine blue–stained cross sections through anthers at different developmental stages of wild-type (Col-0) [(A) to (E)], *35S:MIR156b* [(F) to (J)], *spl8-1* [(K) to (O)] and *35S:MIR156b spl8-1* [(P) to (T)] mutant plants.

(A), (F), (K), and (P) Anthers at stage 2. Within their corners, subepidermal archesporial cells are still detectable or have just undergone a periclinal division to give rise to a PPC and a PSC (arrows).

(B), (G), (L), and (Q) Anthers at stage 3. The PPC and PSC continued to divide to form additional cell layers (arrows) in the wild type (B), *35S:MIR156b* transgenics (G), and *spl8-1* mutants (L). In *35S:MIR156b spl8-1* double mutant plants (Q), this process seems to have come to a hold or to be delayed. (C), (H), (M), and (R) Anthers at stage 4. PSC-derived sporogenous cells are detectable in the center of developing locules surrounded by two cell layers derived from PPCs in the wild type (C), *35S:MIR156b* transgenics (H), and the *spl8-1* mutant (M). Sporogenous cells and structured locule layer formation seem to be absent in *35S:MIR156b spl8-1* plants (R).

(D), (I), (N), and (S) Anthers at stage 5. PMCs are present and surrounded by distinct anther walls in the wild type (D), *35S:MIR156b* transgenics (I), and *spl8-1* mutants (N). Note that the lower left locule of this particular *spl8-1* anther lacks typical PMCs (arrow). Anthers of *35S:MIR156b spl8-1* double mutants (S) lack both the PMCs and the distinct anther walls. Instead, much more vacuolated and connective tissue-like cells occupy their corresponding positions.

(E), (J), (O), and (T) Anthers around stage 12 to 13, carrying pollen grains in each locule, albeit fewer in *35S:MIR156b* transgenics (J) and *spl8-1* mutants (O) compared with the wild type (E). The *35S:MIR156b spl8-1* anther (T) completely lacks pollen sacs, whereas the selected *spl8-1* anther (O) lacks a pollen sac at its inner left side (asterisk).

v, vascular bundle. Bar in the first panel of each column = 25 μ m.

Expression of miR156/7-Targeted *SPL* Genes Becomes Detectable in Anthers of Later Arising Flowers

Our data clearly showed the importance of at least some of the miR156/7-targeted *SPL* genes in early anther development. As *SPL2*, *-11*, *-13*, and *-15* were found to be able to rescue the *spl8* phenotype partially, we selected these as representatives and tried to determine their temporal and spatial expression pattern by RNA in situ hybridization in anthers. To this purpose, apices of wild-type primary inflorescences were fixed at two time points (i.e., after 21 and 30 d of growing in long day) (Figure 6A). At the 21-d time point, the inflorescences had just started to bolt and thus exposed the first floral buds formed. We examined all four miR156/7-targeted *SPL* genes at this time point, and no detectable signal could be observed in young anthers (Figure 6B; see Supplemental Figure 5 online). However, at the 30-d time point and after the inflorescence produced many more flowers, at least *SPL11* could easily be detected in stage 2 anthers (Figure 6C). *SPL11* expression continued to be in the sporogenous tissues at

stage 3 to 4 (Figure 6D) and in PMCs as well as tapetum at stage 5 (Figure 6E), while the expression signal disappeared after meiosis (see Supplemental Figure 5 online). A rather weak signal could also be detected in stage 2 to 4 anthers for *SPL13* (Figures 6F and 6G). Up until stage 7, *SPL13* expression seemed to be mainly restricted to tapetum (Figure 6H). No expression was found in microspores and mature pollen (see Supplemental Figure 5 online). Sporogenous cells of stage 4 anthers also expressed *SPL15* (Figure 6I). Concurrently, a strong signal could be detected for *SPL15* in the inner, placental side of the ovary before ovule initiation. *SPL2* was not easily detected in young anthers, but occasionally sporogenous cells of stage 3 and 4 anthers seemed to react positively (Figures 6J and 6K). As for *SPL11* and *SPL13*, we did not find any expression of *SPL15* and *SPL2* at later (i.e., postmeiotic) anther developmental stages. It should be noted that expression of *SPL8* was found to be similar at both time points and comparable to that shown in Figure 8 (see Supplemental Figure 5 online).

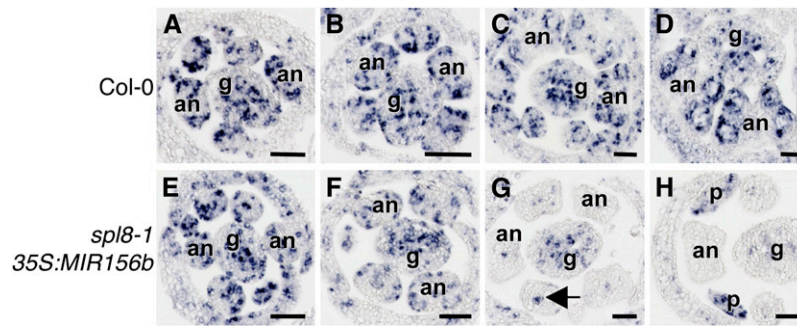


Figure 5. Anther Cell Proliferation Visualized by *H4* in Situ Hybridization.

(A) to (H) Cross sections of flower buds at different developmental stages.

(A) and (E) Stage 2 anthers showing little difference in *H4* hybridization signal between wild-type (A) and *35S:MIR156b spl8-1* (E) plants.

(B) and (F) Stage 3 anthers indicating a diminishing *H4* hybridization signal in *35S:MIR156b spl8-1* (F) in comparison to the wild type (B).

(C) and (G) Stage 5 anthers. *H4* activity remains well detectable and spread in the wild type (C) but has become restricted mainly to the central vasculature in *35S:MIR156b spl8-1* ((G), arrow).

(D) and (H) Stage 6 anthers. *H4* expression continues in the wild type (D) with the developing tapetum showing the strongest signal. By contrast, *35S:MIR156b spl8-1* anthers at this stage are nearly devoid of detectable *H4* activity. Note that *H4* activity also strongly declined in the gynoecium, whereas it is still easily detectable in developing petals.

an, anther; g, gynoecium; p, petal. Bars = 50 μ m.

Our in situ hybridization data demonstrate that at least some of the miR156/7-targeted *SPL* genes are active in early anther development. Interestingly, however, their expression did not seem to become properly established in the first- arising flowers within the primary inflorescence. This would be fully consistent with the observation that the *spl8* mutant does not set seeds in its first flowers despite the likely functional redundancy between *SPL8* and the miR156/7-targeted *SPL* genes in anther development.

MIR156/7 Loci Show Highly Dynamic Expression Patterns during Anther Development

Although expression and function of miR156/7-targeted *SPL* genes seemed to correlate well with early anther development, the role of miR156/7 remained unclear. To gain insight into the temporal and spatial expression of *MIR156/7* loci, we constructed promoter β -glucuronidase (GUS) reporter lines for all 12 *MIR156/7* loci known in the *Arabidopsis* genome (*MIR156a* to *-h* and *MIR157a* to *-d*). After having screened 20 to 30 primary transformants (T1) per construct, we ended up with reproducible GUS activity in different developmental stages and various tissues for 10 out of the 12 loci (for some examples of flower expression patterns, see Supplemental Figure 6 online). For *pMIR156e:GUS* and *pMIR156g:GUS*, no or no consistent GUS staining could be detected. Among the 10 loci showing the GUS signal, *pMIR156a-*, *pMIR156 h-*, *pMIR157c-*, and *pMIR157d:GUS* were found strongly expressed in anthers; *pMIR156 h:GUS* was also expressed in ovules. *pMIR156a:GUS* activity was detected mainly in late anther development and in pollen (see Supplemental Figure 6 online). We selected *pMIR156 h-*, *pMIR157c-*, and *pMIR157d:GUS* lines for further analysis and focused on their expression patterns in cross sections through young an-

thers. Interestingly, a strong GUS signal for all three loci could be detected around meiosis stage. *pMIR156h* and *pMIR157c:GUS* were not detected before anther stage 3 and 4, respectively (Figures 7A, 7B, 7E, and 7F). From stage 4 anthers on, staining in entire anthers increased for *pMIR156 h:GUS* until stages 6 and 7 (Figures 7A, 7C, and 7D). *pMIR157c:GUS* became detectable somewhat later at anther stage 6 (Figures 7E to 7H). Whereas *pMIR157d:GUS* was detected in inflorescence apical meristems and young flower buds containing stage 2 anthers, in stage 3 and 4 anthers, its activity had disappeared (Figures 7I and 7J). A strong GUS signal reappeared in the stage 5 anthers and was maintained through stages 6 and 7 (Figures 7I, 7K, and 7L). For all three loci, the GUS signal was still detectable in anthers immediately after meiosis but vanished within two or three further developmental stages in most cases (see Supplemental Figure 6 online).

To quantify changes in GUS transcript levels in these transgenic plants over time, we harvested the very tip of their primary inflorescences at three successive time points: 25, 40, and 52 d after sowing and cultivation in long days. The transcript levels of *pMIR157c:GUS* and *pMIR157d:GUS* steadily decreased when the plants grew old, whereas the transcript levels first increased and then declined in the *pMIR156h:GUS* lines (Figure 7M). We also compared the temporal GUS reporter transcript patterns to those of the corresponding endogenous pri-miRNA precursors. With the exception of the *pri-miR156h* that remained at a relative high level at 52 d, GUS reporter transcript and *pri-miR* levels were largely consistent (Figure 7N).

Taken together, the GUS reporter lines unveiled a dynamic expression pattern for *MIR156h*, *MIR157c*, and *MIR157d* during early anther development and likely reflected in local miR156/7 levels. Before anther stage 4, low levels of miR156/7 would allow transcribed and targeted *SPL* genes to be fully active at these

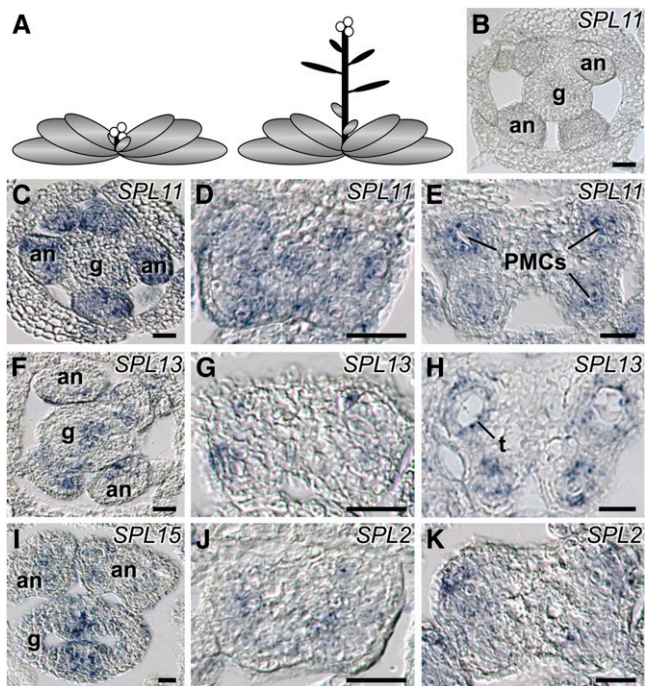


Figure 6. Temporal and Spatial Expression of Selected *SPL* Genes in Anthers.

(A) Graphic representation of plants grown in long days for 21 d (left) and 30 d (right) and used for collecting shoot tips with floral buds for cross-sectioning and in situ hybridization as shown in (B) to (K).

(B) Cross section through one of the earliest flower buds formed in the primary inflorescence (see schematic on the left in [A]) after in situ hybridization with an *SPL11* probe. No detectable expression of *SPL11* was found in these stage 2 anthers.

(C) to (K) Cross sections through buds and anthers of flowers formed relatively late in the primary inflorescence (see schematic on the right in [A]) and hybridized to *SPL* gene probes as indicated below.

(C) Stage 2 anthers (comparable to [B]) showing clear expression of *SPL11*.

(D) Stage 3 anther showing a broad expression of *SPL11* in the anthers.

(E) Stage 5 anther with strongest expression of *SPL11* in pollen mother and tapetal cells.

(F) Stage 2 anthers showing expression of *SPL13*.

(G) Stage 3 anther showing weak *SPL13* expression in sporogenous and parietal cells.

(H) Stage 5 anther expressing *SPL13* mainly in the tapetum.

(I) Stage 4 anthers showing *SPL15* expression in sporogenous cells and the surrounding cell layers. *SPL15* is also clearly expressed in the central placental tissue of the early ovary.

(J) Stage 3 anther showing *SPL2* weakly expressed in sporogenous and parietal cells.

(K) Stage 4 anther expressing *SPL2* in sporogenous cells and surrounding cell layers.

an, anther; g, gynoecium; t, tapetum. Bars = 25 μ m.

stages. The subsequent rise in miR156/7 levels could be required to repress these *SPL* genes below a certain threshold before and during meiosis. As the inflorescence develops, early anthers from late-arising flowers may generally express lower levels of miR156/7 than those arising earlier.

A Relationship between SBP-Box Genes and the Early Anther Gene *SPL/NZZ*

SPL8 together with miR156/7-targeted *SPL* genes promoted sporogenous cell formation, and their complete loss-of-function resulted in loculeless anthers similar to those of *spl/nzz* mutants. To determine a possible interdependency, we examined the expression pattern of *SPL8* and the miR156/7-target *SPL11* in *spl-1* mutant anthers with the help of RNA in situ hybridization. In addition, the expression of *SPL/NZZ* was determined in *spl8-1 35S:MIR156b* plants. In the wild type, the domain of *SPL8* expression covered the four corners of stage 2 anthers where archesporial cells became initiated. Its expression was maintained in PMCs and in the anther walls except the epidermis up until stage 5 (Figures 8A to 8C). In the *spl-1* mutant, the expression domain of *SPL8* seemed to be expanded in stage 2 anthers (Figure 8D), and at later stages, *SPL8* expression could still be detected in the anther lobes (Figures 8E and 8F). In comparison to *SPL8*, *SPL11* seemed to be more broadly expressed in stage 2 and 4 wild-type anthers (Figures 8G and 8H), and later in PMCs and surrounding cell layers at stage 5 (Figure 8I). Strikingly, *SPL11* expression was found to be slightly elevated in young *spl-1* mutant anthers, and the signal appeared to be spread over the entire anther (Figures 8J to 8L). In *spl8-1 35S:MIR156b* transgenic anthers, however, the normal expression of *SPL/NZZ* seemed not to be affected at very early stages of development (Figures 8M and 8P). At later stages, transcript levels of *SPL/NZZ* decreased in the transgenic anthers (Figures 8N and 8Q, and 8O and 8R). Together, these data suggest that *SPL/NZZ* represses the *SPL* genes during early anther development and that these *SPL* genes may not be required for the initiation of *SPL/NZZ* expression.

The miR156/7 Levels Are Reduced in *spl-1* Mutant Inflorescences

As miR156/7-targeted *SPL11* transcript levels seemed to be elevated in *spl-1* mutant anthers, we performed quantitative RT-PCR (qRT-PCR) on inflorescence tips to test if other miR156/7-targeted *SPL* genes were also upregulated in the *spl-1* mutant. In addition to *SPL11*, the related genes *SPL10* and *SPL2* were found to be upregulated more than 1.5 fold. *SPL9* and *SP15* transcript levels were also slightly increased (Figure 9A). We then investigated the possibility that the levels of these different miR156/7-targeted *SPL* transcripts were elevated due to a decrease of miR156/7 in the *spl-1* mutant. We followed the approach described by Yang et al. (2009) and detected mature miR156 and miR157 in the same inflorescence tips (see Methods and the Supplemental Protocol online). Compared with the wild type, the miR156 level in the *spl-1* mutant was decreased 4-fold and the miR157 level 10-fold (Figure 9B). These data support the idea that *SPL/NZZ* represses miR156/7-targeted *SPL* genes through promoting miR156/7, but a more direct repression cannot be ruled out.

DISCUSSION

Using genetic approaches and histologic analyses, we demonstrated a clear role for SBP-box genes in early anther development.

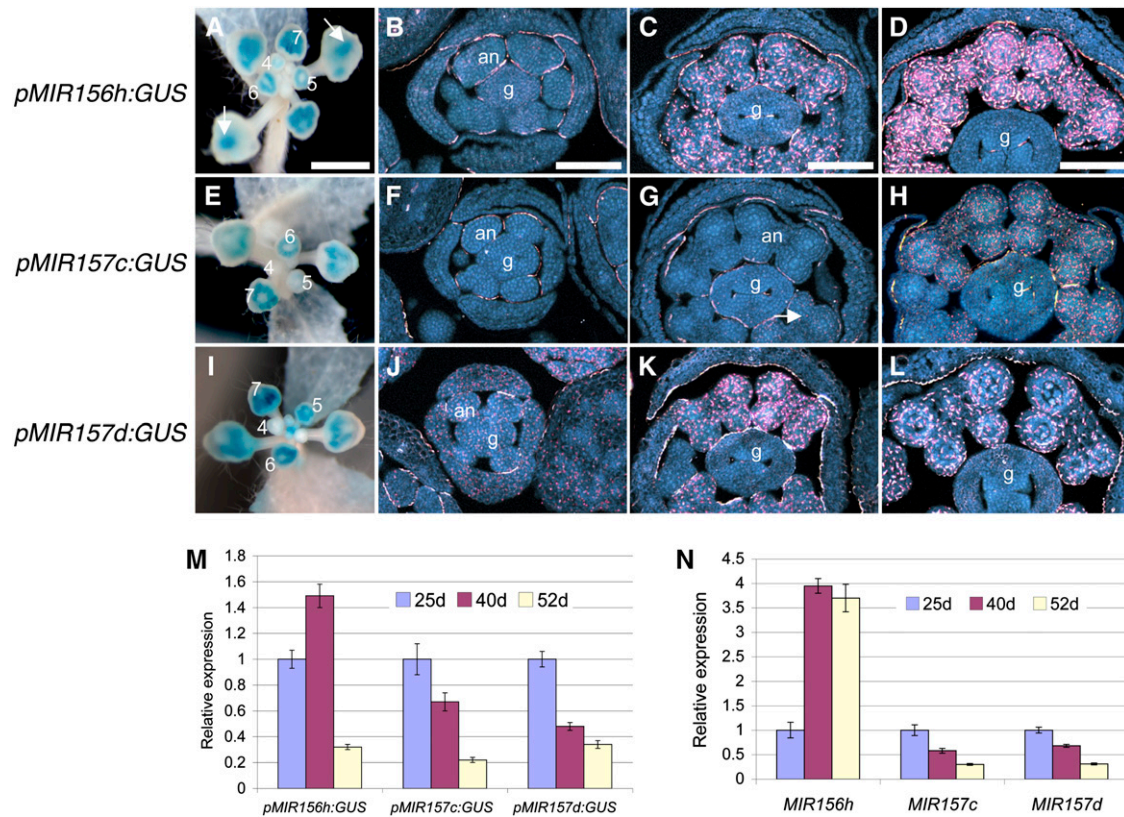


Figure 7. *MIR156/7* Promoter-GUS Reporter Gene Expression at Early Anther Stages.

(A) to (D) *pMIR156h:GUS*.

(E) to (H) *pMIR157c:GUS*.

(I) to (L) *pMIR157d:GUS*.

(A), (E), and (I) Top views of inflorescences from 25-d-old plants with developing flower buds after GUS staining. The numbers indicate the anther stages in these buds. Note that a GUS signal appears in the pistils of *pMIR156h:GUS* flowers during late developmental stages [(A), arrows].

(B) to (D), (F) to (H), and (J) to (L) Transverse sections of early, developing floral buds from 25-d-old plants after GUS staining. Crystalline GUS staining appears pink under dark-field illumination.

(B) Stage 3 anthers with only weak GUS signal detectable.

(C) Stage 5 anthers with GUS signal easily detectable.

(D) Stage 6 anthers with strong GUS signal distributed over the entire anther.

(F) Stage 2 anthers with no GUS signal detectable.

(G) Stage 5 anthers. GUS signal appears in some anthers (arrow).

(H) Stage 6 anthers. GUS signal accumulates widely in all anthers.

(J) Stage 2 anthers. Weak GUS signal detectable in anthers and other floral organs.

(K) Stage 5 anthers. Strong GUS signal distributed over the entire anther.

(L) Stage 7 anthers. GUS signal located mainly in anther walls, but some can be detected in the tetrads as well.

(M) Relative transcript levels of the GUS reporter genes on three time points for *pMIR156h:GUS*, *pMIR157c:GUS*, and *pMIR157d:GUS* transgenic plants.

(N) Relative primary transcript levels of the endogenous *MIR156h*, *MIR157c*, and *MIR157d* loci determined at three different time points.

an, anther; g, gynoecium. Bar in the first panel of each column = 1 mm for (A) and 0.1 mm for (B) to (D). Error bars in (M) and (N) indicate \pm SD ($n = 3$).

The finding that loss- and gain-of-function of selected miR156/7-targeted *SPL* genes enhances or attenuates, respectively, the semisterile phenotype of the *sp18* mutant reveals a degree of functional redundancy among these *SPL* genes.

miR156/7-Targeted *SPL* Genes Are Required for Sporogenous Cell Formation in Anthers

After periclinal division of a subepidermal archesporial cell, the inner daughter cell (i.e., the primary sporogenous cell [PSC])

divides further (anther stage 2 to 4) to give rise to the PMCs seen at stage 5 of anther development. Progeny of the outer daughter cell (i.e., the primary parietal cell [PPC]) become part of the three cell layers (i.e., tapetum, middle layer, and endothecium) surrounding the PMCs (Sanders et al., 1999). In the *sp18* mutant, PMC and parietal cell layer formation failed for some locules but succeeded in others thereby following the wild-type pattern and leading to viable pollen (Unte et al., 2003; this article).

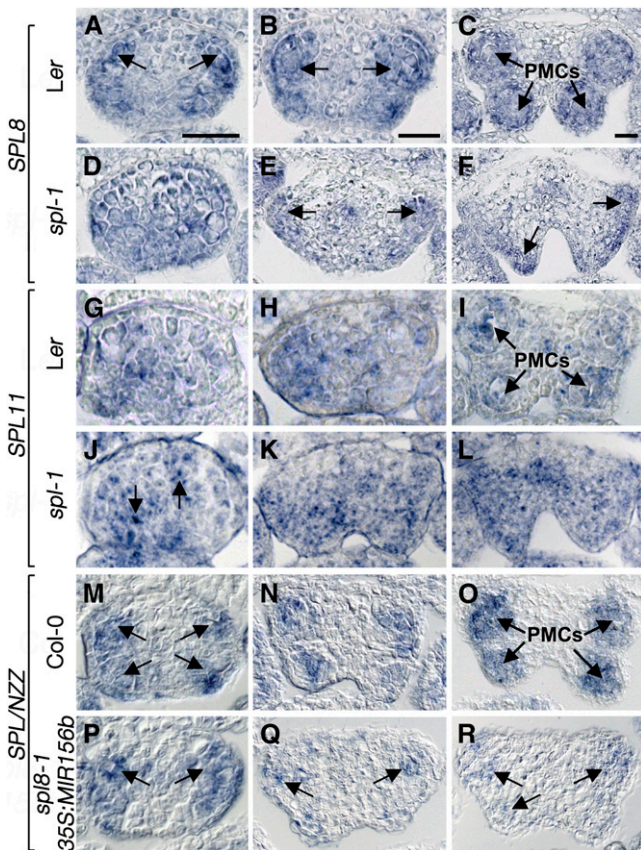


Figure 8. In Situ Hybridization of *SPL8*, *SPL11*, and *SPL/NZZ* mRNA in Early Anthers.

(A) to (C) and (D) to (F) *SPL8* expression in wild-type and *spl-1* mutant anthers, respectively.

(G) to (I) and (J) to (L) *SPL11* expression in wild-type and *spl-1* mutant anthers, respectively.

(M) to (O) and (P) to (R) *SPL/NZZ* expression in wild-type and *spl8-1 35S:MIR156b* mutant anthers, respectively.

(A) and (D) Stage 2 anthers. Whereas expression of *SPL8* is limited mainly to L2-derived cells in the wild type (A, arrows), *spl-1* mutant anthers show a broadened *SPL8* expression domain (D).

(B) and (E) Stage 4 anthers. *SPL8* expression is clearly observed in the sporogenous cells and the parietal cell layers of wild-type anthers (B, arrows), but a less strong and more marginal expression is seen in *spl-1* anthers (E, arrows).

(C) and (F) Stage 5 anthers. *SPL8* expression is detected in PMCs and surrounding cell layers of wild-type anthers (C), and only a weak signal can be found in the corners of abnormal differentiating *spl-1* anthers (F, arrows).

(G) and (J) Stage 2 anthers. Weak *SPL11* expression is found primarily in L2-derived cells of wild-type anthers (G), and a stronger and more spotty hybridization signal seems to occur in *spl-1* anthers (J, arrows).

(H) and (K) Stage 4 anthers. *SPL11* is expressed in the sporogenous cells and surrounding cell layers but not in the epidermis of wild-type anthers (H), and a more spotty signal in *spl-1* anthers seems to be excluded from the abaxial side (K).

(I) and (L) Stage 5 anthers. *SPL11* expression is detected in PMCs and surrounding cell layers of wild-type anthers (I). In *spl-1* mutant anthers, the signals appears stronger and more spotty but outside the abaxial region (L).

A disruption of the earliest stages of pollen sac formation is particularly well known from *spl/nzz* mutants. In *spl/nzz* mutant anthers, archesporial-like cells seem to be specified. However, these cells either do not divide periclinally to form PPCs and PSCs at all (Schieffhale et al., 1999), or else their daughter cells do not give rise to microsporocytes and the different anther wall layers (Yang et al., 1999). This phenotype is very similar to what we observed after downregulation of miR156/7-targeted *SPL* genes by overexpressing *MIR156b* in the *spl-1* mutant. In this case as well, archesporial-like cells seem to appear and to divide but the PPC- and PSC-like daughter cells cannot form the typical anther wall layers and microsporocytes. As a result, small anthers develop, fully occupied with vacuolated cells (Figures 4P to 4T).

These phenotypic similarities between *spl/nzz* and *spl8 35S:MIR156b* plants imply that these genes are involved in the same pathway for regulating pollen sac formation in early anther development. RNA in situ hybridization results suggest that *SPL8* and *SPL/NZZ* become independently activated in stage 2 anthers. *SPL/NZZ* then seems to keep *SPL8* expression restricted to the four corners of the anther. In *spl-1* mutant anthers comparable to stage 4 to 5 in the wild type, tissues do not differentiate properly and *SPL8* is found to be slightly down-regulated. Similarly, *SPL/NZZ* is also slightly down-regulated in anthers of the comparable stage in *spl8-1 35S:MIR156b* flowers. Furthermore, we observed that a *SPL-GUS* reporter transgene remains strongly expressed in the whole anther during its entire development in *spl8-1 35S:MIR156b* flowers (see Supplemental Figure 7 online). Together, these data show that sporogenous tissues do not form in the absence of *SPL8* and other miR156/7-targeted *SPL* genes and that these genes are required for *SPL/NZZ* to act in promoting sporogenous cell formation.

Both male and female organs express *SPL/NZZ* during early and late stages (Schieffhale et al., 1999; Yang et al., 1999). Likewise, the expression of *SPL8* and other miR156/7-targeted *SPL* genes can also be detected in both male and female organs, consistent with an important role in reproductive organ development. However, in anthers, their expression remains restricted mainly to early stages (i.e., before meiosis), whereas *SPL/NZZ* activity can still be observed thereafter during pollen development (Dinneny et al., 2006).

As a direct target of the floral organ homeotic gene *AG*, and based on its dramatic mutant phenotype, *SPL/NZZ* is considered one of earliest genes required for initiation of micro- and

(M) and (P) Stage 2 anthers. *SPL/NZZ* expression is seen in L2-derived cells in the four corners of both wild-type (M, arrows) and *spl8-1 35S:MIR156b* anthers (P, arrows).

(N) and (Q) Stage 4 anthers. *SPL/NZZ* is expressed in the sporogenous cells of the four lobes in wild-type anthers (N). However, markedly weaker signal is found in those of *spl8-1 35S:MIR156b* anthers (Q, arrows).

(O) and (R) Stage 5 anthers. *SPL/NZZ* expression is easily detectable in PMCs and surrounding cell layers of wild-type anthers (O), but only a very weak signal can be seen in the four lobes of *spl8-1 35S:MIR156b* anthers (R, arrows).

Bar in the first panel of each column = 25 μ m.

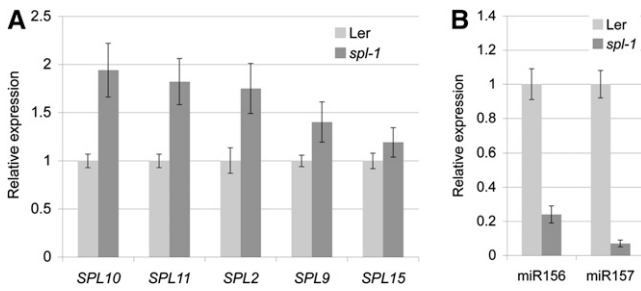


Figure 9. Comparative Expression Levels of miR156/7 and Several of Their Targets in the Wild Type and the *spl-1* Mutant.

Relative expression levels as determined by qRT-PCR on RNA from inflorescence apices of 40-d-old plants grown in long days, representing floral buds up until stage 12 (Smyth et al., 1990).

(A) Relative expression levels of miR156/7-targeted *SPL* genes in the wild type (*Ler*) and *spl-1*.

(B) Relative expression levels of mature miR156 and miR157 in the wild type (*Ler*) and *spl-1*.

Error bars indicate \pm SD ($n = 3$).

megasporogenesis. Despite its fundamental role in *Arabidopsis* fertility, both maize (*Zea mays*) and rice (*Oryza sativa*) seem to lack true *SPL/NZZ* homologs (Ma et al., 2007; GenBank, July 2010). This strongly suggests that sporogenous cell formation in these, and probably other monocots, requires another regulator (s). A *SPL/NZZ*-like function in maize anthers may be fulfilled by *MSCA1*. The *mzca1* mutant also lacks sporogenous cell formation, although archesporial cells seem to become specified in its anthers (Chaubal et al., 2003).

Interesting in this context is that both miR156/7-targeted and nontargeted SBP-box genes, which according to our data regulate anther development similarly and as early as *SPL/NZZ*, are well conserved between monocots and dicots (Xie et al., 2006; Riese et al., 2007; Hultquist and Dorweiler, 2008). It would thus be interesting to determine if SBP-box genes play an evolutionarily more conserved role in sporogenesis. A difficulty may be that due to a high degree of functional redundancy, loss of function of one or two genes within this group may cause only minor fertility defects, as seen in *Arabidopsis*.

miR156/7-Targeted *SPL* Genes Promote Cell Proliferation

Cell proliferation is an important determinant of organ patterning and growth, which relies on many coordinated regulation factors, including cell cycle genes and other developmental factors (Rodriguez et al., 2010; Sozzani et al., 2010). Several lines of evidence indicate that *SPL* genes promote cell proliferation. The *mcs-1D* mutant, representing a miR156-resistant *spl15* mutant allele gene, shows increased cell number and decreased cell size in leaves. Overexpression of *SPL3* also increases cell number and decreases cell size in leaves. By contrast, overexpression of miR156 results in the opposite (Usami et al., 2009). The *spl8-1* mutant, displaying larger cotyledons and young leaves with reduced cell numbers and increased cell sizes, provides another example. Overexpression of *SPL8* leads again to the opposite phenotype (Zhang, 2005). Here, we used the cell proliferation

marker *H4* to show that *SPL8* and miR156/7-targeted *SPL* genes are required for maintaining cell proliferation in early anthers (Figure 5). Taken together, these data clearly point to a role for *SPL* genes in cell proliferation, but the molecular genetic mechanisms involved need to be clarified.

miR156/7 Levels Follow Complex Spatial and Temporal Changes in Anthers

Recent studies demonstrated that variation in the level of miR156 and its targets is sufficient to promote or delay the juvenile-to-adult development in *Arabidopsis* (Wu and Poethig, 2006; Schwarz et al., 2008; Wang et al., 2009; Wu et al., 2009). Starting high in young seedlings, the overall miR156 level declines as plants grow (Wang et al., 2009; Wu et al., 2009). By contrast, the targeted *SPL* genes exhibit an opposite expression pattern. During the reproductive phase, flowers form with more complex tissues and organs and determining miR156/7 expression patterns in these developing floral organs is not an easy task, although in situ hybridization can be applied (Válóczi et al., 2006; Wang et al., 2008). Moreover, several different loci are able to contribute to miR156/7 levels. To get an impression of miR156/7 distribution during plant development, we generated transgenic

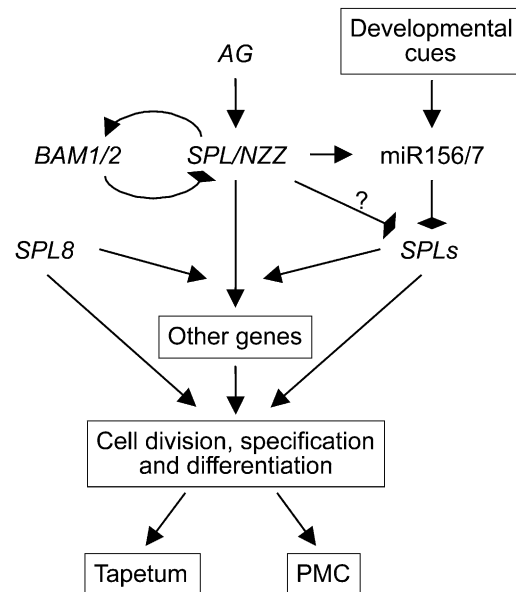


Figure 10. A Model for *SPL8* and miR156/7-Targeted *SPL* Gene Function in Early Anther Development in *Arabidopsis*.

At the onset of the anther developmental program, the floral C function gene *AG* promotes the expression of *SPL/NZZ*. *SPL/NZZ* is required for proper expression of genes involved in cell division, differentiation, and specification and leads to PMC and tapetum formation. Equally critical at this stage appear to be the *SPL8* and miR156/7-targeted *SPL* gene functions, either required to act together with *SPL/NZZ* or independently to regulate genes mediating cell division, differentiation, and specification. Lines ending with arrowheads indicate positive and those with rhombs negative genetic interactions. A question mark indicates a possible but yet unclear interaction.

GUS reporter lines for the different *MIR156/7* loci. Different organs at different stages of development showed highly dynamic expression patterns (see Supplemental Figure 6 online). Also, different loci showed overlap in expression in both time and space, suggesting some functional redundancy. For example, expression of *MIR157a* and *-b*, predicted to encode identical miRNAs, as well as the slightly different miRNA-encoding *MIR156a*, could be detected in late stages of pollen development (see Supplemental Figure 6 online). Overall, the GUS staining patterns obtained imply that the miR156/7 levels in different tissues and organs vary; accordingly, transcript levels of the targeted *SPL* genes are affected. In anther development, we found that expression of *MIR156h* and *MIR157c* and *-d* coincided with that of their targets around meiosis. This could mean that instead of fully repressing their targets, miR156/7 action at these stages involves fine tuning target transcript levels, a mode of action shown for some other conserved plant miRNAs (Cartolano et al., 2007). A study of *MIR156/7* mutants is required to reveal the degree of redundancy and their mode of action.

SPL/NZZ Represses miR156/7-Targeted SPL Genes in Anthers

Our results demonstrated that *SPL8*, in concert with miR156/7-targeted *SPL* genes, affects sporogenous cell and parietal cell formation very similarly to *SPL/NZZ*. However, it remains unknown if these genes are involved in the same pathway in regulating this process. A transcriptome analysis showed that both *SPL/NZZ*-dependent and -independent transcriptional programs are required for normal anther development (Wijeratne et al., 2007). Mutation of *SPL/NZZ* leads to a fold change of two or more of ~2000 genes on the level of transcription. Which of these represent direct targets of *SPL/NZZ* remains unknown. Interestingly, *in situ* hybridization showed that *SPL11* was upregulated in the *spl-1* mutant, a finding further supported with the help of qRT-PCR. The latter approach also revealed upregulation of other miR156/7-targeted *SPL* genes, such as *SPL10*, *-2*, *-9*, and *-15* in the *spl/nzz* mutant. Our findings here are consistent with the published microarray data of Wijeratne et al. (2007), who reported upregulation of *SPL11*, *-10*, *-5*, and *-15* in the *spl-1* mutant. Taken together, the available data strongly supports the hypothesis that *SPL/NZZ* represses miR156/7-targeted *SPL* genes in anthers. As multiple and different miR156/7-targeted *SPL* genes are involved, it might well be that *SPL/NZZ* is actually repressing these genes through miR156/7. In fact, this assumption finds support in our qRT-PCR data showing that both miR156 and miR157 levels were reduced in the *spl-1* mutant.

Our qRT-PCR data indicated that expression of *MIR157c* and *MIR157d* was downregulated but that of *MIR156h* upregulated in the *spl-1* mutant (see Supplemental Figure 8 online). Whether *SPL/NZZ* is involved in general miRNA biogenesis or directly represses the *MIR156/7* genes thus remains to be determined. Furthermore, we cannot rule out the possibility that *SPL/NZZ* directly represses miR156/7-targeted *SPL* genes, particularly in the first formed flowers where we did not detect expression of these *SPL* genes in early anther development (Figure 6B).

A Model for Function of SBP-Box Genes in Early Anther Development

The *SPL/NZZ* gene plays a key role in early anther development by promoting other early anther genes required for cell division, specification, and differentiation, resulting in PMC and tapetum formation (Schiefthaler et al., 1999; Yang et al., 1999). The *SPL/NZZ* gene is a direct target of the floral C function gene *AG* (Ito et al., 2004) and, based on its expression profile, clusters with *SPL8* during early flower development (i.e., flower stages 5 to 7 [Wellmer et al., 2006] representing anther stages 1 to 3 [Sanders et al., 1999]).

Based on these facts together with the data presented in this study, we propose a model to integrate the function of *SPL8* and miR156/7-targeted *SPL* genes in early anther development (Figure 10). In this model, it is assumed that the latter SBP-box genes, with the possible exception of *SPL3*, *-4*, *-5*, and *-6*, act redundantly to enable *SPL/NZZ* to activate its targets involved in cell proliferation and differentiation. They may, as well, act directly on the same targets. At these early stages, *SPL/NZZ* promotes *BAM1* and *-2* expression; in turn, the latter restricts *SPL/NZZ* expression to the center of the developing pollen sac (Hord et al., 2006; Wijeratne et al., 2007). Furthermore, *SPL/NZZ* is assumed to promote miR156/7 levels at later stages of anther development. In the first several arising flowers, miR156/7-targeted *SPL* gene expression remains insufficient, possibly as a result of a still too high miR156/7 level in anthers as a remnant related to the preceding floral transition. Thus, *SPL8* is absolutely required for proper early anther development during early inflorescence development. Mutation of *SPL8* at this stage results in a severe sterile flower phenotype. Further decline of miR156/7 or other repressor levels will then allow miR156/7-targeted *SPL* transcripts start to accumulate in the flowers initiated at somewhat later stages of inflorescence development. At this stage, loss of *SPL8* function is thus partially compensated for by these other SBP-box genes and fertility is only moderately affected (Figures 1C and 1D).

Obviously, this model will need elaboration and refinement, in particular when more detailed knowledge on the regulation of miR156/7, their SBP-box gene targets and targets thereof, becomes available.

METHODS

Plant Materials and Growth Conditions

Arabidopsis thaliana ecotypes Columbia (Col-0) or Landsberg *erecta* (*Ler*) were used as wild-type controls as indicated per experiment. All mutants and transgenics are in the Col-0 background with the exception of *spl-1*, which is in the *Ler* background (N6586; Nottingham Arabidopsis Stock Centre). *spl8* single mutants (Unte et al., 2003), the *spl2-1 spl9-1 spl15-1* triple mutant (Schwarz et al., 2008), and the *35S:MIR156a* (Wu and Poethig, 2006) and *35S:MIR156b* (Schwab et al., 2005) transgenic lines have been described before. Seeds were imbibed and stratified for 4 d in the dark at 4°C prior to sowing. Plants were cultivated on prefertilized soil mixture (Type ED73; Werkverband) at 21 to 23°C under long-day conditions (16 h light) in the greenhouse. For comparative experiments, plants were grown in parallel under the same conditions, and material for gene expression studies was harvested at the same time points.

Plasmid Construction and Plant Transformation

For complementation of the *sp18* mutant, a fragment encompassing a 2.1-kb upstream promoter region, a 1002-bp cDNA (open reading frame [ORF]) encoding full-size SPL8 protein, and a 190-bp 3'-untranslated region fragment of *SPL8* was inserted into the binary vector pGSA1252 (www.chromdb.org) by replacing the 35S promoter and GUS intron following *Bgl*III and *Spe*I digestion. The resulting plasmid is referred to as *pSPL8:SPL8*. The miR156/7-resistant *rSPL2*, *rSPL11*, *rSPL9*, *rSPL15*, *rSPL6*, and *rSPL13* transgenes were generated by introducing mutations into the predicted miR156 response elements (see Supplemental Table 1 online) using recombinant PCR. For the generation of *rSPL3*, only its ORF was amplified omitting the miR156 response element in its 3'-untranslated region. The respective transgenes were subcloned into the *pSPL8:SPL8* plasmid by replacing the *SPL8* ORF following digestion with *Sma*I and either *Sac*I or *Xba*I, resulting in plasmids referred to as *pSPL8:rSPL3*, *pSPL8:rSPL2*, *pSPL8:rSPL11*, *pSPL8:rSPL9*, *pSPL8:rSPL15*, *pSPL8:rSPL6*, and *pSPL8:rSPL13*. The GUS reporter constructs representing the various *MIR156/7* loci resulted from amplification of ~2.5-kb upstream promoter region of the respective loci followed by cloning into the pGPTV-bar binary vector (Becker et al., 1992) linearized using *Sma*I and *Xba*I. To generate the *p35S:MIR156h* construct, a 450-bp genomic fragment encompassing the miR156h encoding region was amplified and cloned into the pBAR-35S vector (Xing et al., 2005) linearized using *Sma*I and *Xba*I. Oligonucleotides for mutagenesis and other PCRs used in generating the plasmids mentioned above are listed in Supplemental Table 2 online. All constructs were validated by sequencing before transforming into *sp18-1* or *sp18-3* mutants or wild-type plants, respectively, by the floral dipping method (Clough and Bent, 1998).

In Situ Hybridization

RNA in situ hybridization was performed as described previously (Xing et al., 2005). To generate antisense probes and to avoid cross-hybridization among *SPL* gene transcripts, only cDNA sequences downstream of the SBP-box from *SPL2*, *SPL11*, *SPL13*, and *SPL15* were amplified. For *SPL8*, a fragment upstream of the SBP-box was added to a downstream fragment. Generation of an *SPL/NZZ* antisense probe was done as described previously (Xing and Zachgo, 2008). All primers used for the amplification of the probes referred to above, as well as for an antisense *H4* probe, are listed in Supplemental Table 2 online (with the presence of a T3 or T7 RNA polymerase binding motif indicated in lowercase). T7 RNA polymerase (Roche) was used for in vitro transcription.

Histology and Microscopy

For comparative anther histology, the young floral buds representing different developmental stages were processed and sectioned as described by Sorensen et al. (2002). Transgenic GUS-expressing plant material was stained following the protocol of Müller et al. (2001) and analyzed using a Leica MZFLIII fluorescence stereomicroscope. For preparation of semithin sections through GUS-stained floral buds, samples were dehydrated in an increasing ethanol series (70, 96, 100%, v/v). Samples were then stepwise infiltrated with Technovit 7100 (Heraeus Kulzer) via a 3:1, 1:1, and 1:3 ethanol:Technovit series by incubating for 45 min at each step. Finally, the samples were incubated overnight in pure Technovit at room temperature. Technovit preparation and polymerization were done according to the manufacturer's protocol. One- to three-micrometer-thick sections were prepared using a Reichert ultramicrotome and mounted with entalan. All sectioned material was observed under a Zeiss Axiophot microscope. GUS precipitates were visualized using dark-field optics in combination with UV epifluorescence

to visualize the tissue. Micrographs were recorded using a Leica DFC490 digital camera.

To determine pollen production, 30 unopened anthers were dissected from different flowers just before dehiscence and collected in Eppendorf tubes. Pollen were released by homogenizing in 20% glycerol and 1× PBS, pH 7, buffer (gly-PBS), pelleted by centrifugation, and resuspended in 100 μL gly-PBS containing 1% lacto-phenol fuchsin stain. Droplets of 5 μL were pipetted on microscopy slides covered with semidry 1% agarose to absorb the liquid, thereby generating flat spots of ~4 mm in diameter. These were photographed entirely and the fluorescing pollen grains counted using the public domain software ImageJ (Wayne Rasband, National Institutes of Health). Seed set was determined by clearing advanced but unopened siliques in Hoyer's solution and counting seeds directly under the stereomicroscope. To check pollen sac number in anthers, 8-μm-thick transverse sections were prepared from whole flower buds after dehydration and embedding in paraffin.

Real-Time qRT-PCR

Total RNA from inflorescence tips, carrying stage 1 to 12 floral buds, was isolated using the RNeasy plant mini kit (Qiagen). Five micrograms of total RNA, treated with DNase I, were used for first-strand cDNA synthesis with Superscript III (Invitrogen). qPCR master mix was prepared using the IQ SYBR Green Supermix (Bio-Rad) with specific primers for *SPL2*, *SPL9*, *SPL10*, *SPL11*, and *SPL15* genes and *MIR156h*, *MIR157c*, and *MIR157d* precursors. PCR reactions were run and analyzed using the Bio-Rad IQ5 sequence detection system. Results were normalized to the expression of *PP2A* (Czechowski et al., 2005) mRNA. For determination of mature miR156/7 levels, total RNA was extracted using the mirVana miRNA isolation kit (Ambion). After the DNase I treatment, 200 ng of RNA were taken for cDNA synthesis with specific RT primers designed according to Yang et al. (2009). However, detection in the subsequent qRT-PCR relied on SYBR green instead of TaqMan technology as originally described by these authors (see Supplemental Protocol online). All specific primers used are listed in Supplemental Table 2 online. Representative qRT-PCR data of one of two to three independent biological replicates are presented in the figures with error bars representing the SD of three technical replicates.

Phylogenetic Tree Construction

Multiple alignments of protein sequences and phylogenetic reconstructions were performed by the program ClustalW and the neighbor-joining algorithm, both at default settings, within the MacVector 9.5.2 software package. MacVector's Best tree mode output was converted to the radial unrooted phylogram shown in Figure 1A using Dendroscope (Huson et al., 2007). MacVector's Bootstrap mode output with 10,000 replications was used to identify branching points that occurred in >50% of the resampling trees. For alignment and reconstruction, the SBP domain of 74-amino acid residues was used with two additional downstream residues (cf. to sequence logo provided in Birkenbihl et al., 2005). The alignment is available as Supplemental Data Set 1 online.

Remaining Techniques and Image Processing

Standard molecular biology techniques were performed as described by Sambrook et al. (1989). Graphical plots of numerical data were generated with Excel (Microsoft Germany), and statistical tests were performed using the Student's *t* test within this program. P values lower than 0.05 were considered to be statistically relevant. Digital photographic images were cropped using Adobe Photoshop CS (Adobe Systems). Color and contrast corrections were performed on entire images only. Figures were assembled in PowerPoint (Microsoft Germany).

Accession Numbers

Sequence data from this article can be found in the Arabidopsis Genome Initiative or GenBank/EMBL databases under the following accession numbers: At1g02065 (*SPL8*), At5g43270 (*SPL2*), At2g33810 (*SPL3*), At1g69170 (*SPL6*), At2g42200 (*SPL9*), At1g27360 (*SPL11*), At5g50570 (*SPL13A*), At5g50670 (*SPL13B*), At3g57920 At5g50570 (*SPL15*), At4g27330 (*SPL/NZZ*), At2g25095 (*MIR156a*), At4g30972 (*MIR156b*), At4g31877 (*MIR156c*), At5g10945 (*MIR156d*), At5g11977 (*MIR156e*), At5g26147 (*MIR156f*), At2g19425 (*MIR156g*), At5g55835 (*MIR156h*), At1g66783 (*MIR157a*), At1g66795 (*MIR157b*), At3g18217 (*MIR157c*), At1g48742 (*MIR157d*), and At1g07820 (*Histone H4*).

Supplemental Data

The following materials are available in the online version of this article.

Supplemental Figure 1. Relative Expression of the miR156-Targeted *SPL* Genes in 35S:*MIR156b* Transgenic Plants.

Supplemental Figure 2. Relative Expression of Selected miR156-Targeted *SPL* Genes in *sp18-1 MIM156* Plants.

Supplemental Figure 3. Variation in Relative Transgene Expression among Different *pSPL8:rSPL13* Transgenic Lines.

Supplemental Figure 4. Histological Analysis of *sp18-1 spl2-1 spl9-1 spl15-1* Quadruple Mutant Anthers.

Supplemental Figure 5. Temporal and Spatial Expression of Selected *SPL* Genes in Anthers.

Supplemental Figure 6. Different *MIR156/7* Loci Promoter-Driven *GUS* Reporter Gene Expression Patterns in Flowers.

Supplemental Figure 7. *SPL/NZZ*-Driven *GUS* Reporter Gene Expression in Inflorescences.

Supplemental Figure 8. Comparative Expression Levels of *MIR156h*, *MIR157c*, and *MIR157d* in the Wild Type and the *sp1-1* Mutant.

Supplemental Table 1. Nucleotide Mutations in the miR156 Response Elements of *rSPL* Transgenes.

Supplemental Table 2. Oligonucleotide Primer Sequences.

Supplemental Data Set 1. Text File (NEXUS Format) of the Alignment Used to Generate the Phylogram Shown in Figure 1A.

Supplemental Protocol. Detection and Quantification of miR156/7 Using qRT-PCR in *Arabidopsis*

ACKNOWLEDGMENTS

We thank the Weigel laboratory (Max-Planck-Institut für Entwicklungsbiologie, Tübingen, Germany) for providing the 35S:*MIR156b* and *MIM156* transgenic lines, the Poethig laboratory (University of Pennsylvania, Philadelphia, PA) for the 35S:*MIR156a* line, and the Yanofsky laboratory (University of California at San Diego, La Jolla, CA) for the *SPL-GUS* reporter line. This project was funded by the Deutsche Forschungsgemeinschaft through SFB572.

Received September 6, 2010; revised November 19, 2010; accepted December 3, 2010; published December 21, 2010.

REFERENCES

Albrecht, C., Russinova, E., Hecht, V., Baaijens, E., and de Vries, S. (2005). The *Arabidopsis thaliana* SOMATIC EMBRYOGENESIS RE-

CEPTOR-LIKE KINASES1 and 2 control male sporogenesis. *Plant Cell* **17**: 3337–3349.

Alves-Ferreira, M., Wellmer, F., Banhara, A., Kumar, V., Riechmann, J.L., and Meyerowitz, E.M. (2007). Global expression profiling applied to the analysis of *Arabidopsis* stamen development. *Plant Physiol.* **145**: 747–762.

Arazi, T., Talmor-Neiman, M., Stav, R., Riese, M., Huijser, P., and Baulcombe, D.C. (2005). Cloning and characterization of micro-RNAs from moss. *Plant J.* **43**: 837–848.

Becker, D., Kemper, E., Schell, J., and Masterson, R. (1992). New plant binary vectors with selectable markers located proximal to the left T-DNA border. *Plant Mol. Biol.* **20**: 1195–1197.

Birkenbihl, R.P., Jach, G., Saedler, H., and Huijser, P. (2005). Functional dissection of the plant-specific SBP-domain: overlap of the DNA-binding and nuclear localization domains. *J. Mol. Biol.* **352**: 585–596.

Canales, C., Bhatt, A.M., Scott, R., and Dickinson, H. (2002). EXS, a putative LRR receptor kinase, regulates male germline cell number and tapetal identity and promotes seed development in *Arabidopsis*. *Curr. Biol.* **12**: 1718–1727.

Cardon, G., Höhmann, S., Klein, J., Nettesheim, K., Saedler, H., and Huijser, P. (1999). Molecular characterisation of the *Arabidopsis* SBP-box genes. *Gene* **237**: 91–104.

Cardon, G.H., Höhmann, S., Nettesheim, K., Saedler, H., and Huijser, P. (1997). Functional analysis of the *Arabidopsis thaliana* SBP-box gene *SPL3*: A novel gene involved in the floral transition. *Plant J.* **12**: 367–377.

Cartolano, M., Castillo, R., Efremova, N., Kuckenberger, M., Zethof, J., Gerats, T., Schwarz-Sommer, Z., and Vandenbussche, M. (2007). A conserved microRNA module exerts homeotic control over *Petunia hybrida* and *Antirrhinum majus* floral organ identity. *Nat. Genet.* **39**: 901–905.

Chaubal, R., Anderson, J.R., Trimmell, M.R., Fox, T.W., Albertsen, M.C., and Bedinger, P. (2003). The transformation of anthers in the *msc1* mutant of maize. *Planta* **216**: 778–788.

Clough, S.J., and Bent, A.F. (1998). Floral dip: A simplified method for *Agrobacterium*-mediated transformation of *Arabidopsis thaliana*. *Plant J.* **16**: 735–743.

Colcombet, J., Boisson-Dernier, A., Ros-Palau, R., Vera, C.E., and Schroeder, J.I. (2005). *Arabidopsis* SOMATIC EMBRYOGENESIS RECEPTOR KINASES1 and 2 are essential for tapetum development and microspore maturation. *Plant Cell* **17**: 3350–3361.

Czechowski, T., Stitt, M., Altmann, T., Udvardi, M.K., and Scheible, W.R. (2005). Genome-wide identification and testing of superior reference genes for transcript normalization in *Arabidopsis*. *Plant Physiol.* **139**: 5–17.

Dinneny, J.R., Weigel, D., and Yanofsky, M.F. (2006). *NUBBIN* and *JAGGED* define stamen and carpel shape in *Arabidopsis*. *Development* **133**: 1645–1655.

Franco-Zorrilla, J.M., Valli, A., Todesco, M., Mateos, I., Puga, M.I., Rubio-Somoza, I., Leyva, A., Weigel, D., Garcia, J.A., and Paz-Ares, J. (2007). Target mimicry provides a new mechanism for regulation of microRNA activity. *Nat. Genet.* **39**: 1033–1037.

Gandikota, M., Birkenbihl, R.P., Höhmann, S., Cardon, G.H., Saedler, H., and Huijser, P. (2007). The miRNA156/157 recognition element in the 3' UTR of the *Arabidopsis* SBP box gene *SPL3* prevents early flowering by translational inhibition in seedlings. *Plant J.* **49**: 683–693.

Hennig, L., Gruijsem, W., Grossniklaus, U., and Köhler, C. (2004). Transcriptional programs of early reproductive stages in *Arabidopsis*. *Plant Physiol.* **135**: 1765–1775.

Hord, C.L., Chen, C., Deyoung, B.J., Clark, S.E., and Ma, H. (2006). The BAM1/BAM2 receptor-like kinases are important regulators of *Arabidopsis* early anther development. *Plant Cell* **18**: 1667–1680.

- Hultquist, J.F., and Dorweiler, J.E. (2008). Feminized tassels of maize *mop1* and *ts1* mutants exhibit altered levels of miR156 and specific SBP-box genes. *Planta* **229**: 99–113.
- Husbands, A.Y., Chitwood, D.H., Plavskin, Y., and Timmermans, M.C. (2009). Signals and prepatterning: New insights into organ polarity in plants. *Genes Dev.* **23**: 1986–1997.
- Huson, D.H., Richter, D.C., Rausch, C., DeZulian, T., Franz, M., and Rupp, R. (2007). Dendroscope: An interactive viewer for large phylogenetic trees. *BMC Bioinformatics* **8**: 460.
- Ito, T., Wellmer, F., Yu, H., Das, P., Ito, N., Alves-Ferreira, M., Riechmann, J.L., and Meyerowitz, E.M. (2004). The homeotic protein AGAMOUS controls microsporogenesis by regulation of *SPOROCYTELESS*. *Nature* **430**: 356–360.
- Jia, G., Liu, X., Owen, H.A., and Zhao, D. (2008). Signaling of cell fate determination by the TPD1 small protein and EMS1 receptor kinase. *Proc. Natl. Acad. Sci. USA* **105**: 2220–2225.
- Jiao, Y., Wang, Y., Xue, D., Wang, J., Yan, M., Liu, G., Dong, G., Zeng, D., Lu, Z., Zhu, X., Qian, Q., and Li, J. (2010). Regulation of *OsSPL14* by OsmiR156 defines ideal plant architecture in rice. *Nat. Genet.* **42**: 541–544.
- Klein, J., Saedler, H., and Huijser, P. (1996). A new family of DNA binding proteins includes putative transcriptional regulators of the *Antirrhinum majus* floral meristem identity gene *SQUAMOSA*. *Mol. Gen. Genet.* **250**: 7–16.
- Kropat, J., Tottey, S., Birkenbihl, R.P., Depège, N., Huijser, P., and Merchant, S. (2005). A regulator of nutritional copper signaling in *Chlamydomonas* is an SBP domain protein that recognizes the GTAC core of copper response element. *Proc. Natl. Acad. Sci. USA* **102**: 18730–18735.
- Liu, X., Huang, J., Parameswaran, S., Ito, T., Seubert, B., Auer, M., Rymaszewski, A., Jia, G., Owen, H.A., and Zhao, D. (2009). The *SPOROCYTELESS/NOZZLE* gene is involved in controlling stamen identity in *Arabidopsis*. *Plant Physiol.* **151**: 1401–1411.
- Lu, X.C., Gong, H.Q., Huang, M.L., Bai, S.L., He, Y.B., Mao, X., Geng, Z., Li, S.G., Wei, L., Yuwen, J.S., Xu, Z.H., and Bai, S.N. (2006). Molecular analysis of early rice stamen development using organ-specific gene expression profiling. *Plant Mol. Biol.* **61**: 845–861.
- Ma, H. (2005). Molecular genetic analyses of microsporogenesis and microgametogenesis in flowering plants. *Annu. Rev. Plant Biol.* **56**: 393–434.
- Ma, J., Duncan, D., Morrow, D.J., Fernandes, J., and Walbot, V. (2007). Transcriptome profiling of maize anthers using genetic ablation to analyze pre-meiotic and tapetal cell types. *Plant J.* **50**: 637–648.
- Ma, J., Skibbe, D.S., Fernandes, J., and Walbot, V. (2008). Male reproductive development: Gene expression profiling of maize anther and pollen ontogeny. *Genome Biol.* **9**: R181.
- Manning, K., Tör, M., Poole, M., Hong, Y., Thompson, A.J., King, G.J., Giovannoni, J.J., and Seymour, G.B. (2006). A naturally occurring epigenetic mutation in a gene encoding an SBP-box transcription factor inhibits tomato fruit ripening. *Nat. Genet.* **38**: 948–952.
- Martin, R.C., Liu, P.P., Goloviznina, N.A., and Nonogaki, H. (2010). microRNA, seeds, and Darwin?: Diverse function of miRNA in seed biology and plant responses to stress. *J. Exp. Bot.* **61**: 2229–2234.
- Miura, K., Ikeda, M., Matsubara, A., Song, X.J., Ito, M., Asano, K., Matsuoka, M., Kitano, H., and Ashikari, M. (2010). *OsSPL14* promotes panicle branching and higher grain productivity in rice. *Nat. Genet.* **42**: 545–549.
- Mizuno, S., Osakabe, Y., Maruyama, K., Ito, T., Osakabe, K., Sato, T., Shinozaki, K., and Yamaguchi-Shinozaki, K. (2007). Receptor-like protein kinase 2 (RPK 2) is a novel factor controlling anther development in *Arabidopsis thaliana*. *Plant J.* **50**: 751–766.
- Moreno, M.A., Harper, L.C., Krueger, R.W., Dellaporta, S.L., and Freeling, M. (1997). *liguleless1* encodes a nuclear-localized protein required for induction of ligules and auricles during maize leaf organogenesis. *Genes Dev.* **11**: 616–628.
- Müller, A., Iser, M., and Hess, D. (2001). Stable transformation of sunflower (*Helianthus annuus* L.) using a non-meristematic regeneration protocol and green fluorescent protein as a vital marker. *Transgenic Res.* **10**: 435–444.
- Reinhart, B.J., Weinstein, E.G., Rhoades, M.W., Bartel, B., and Bartel, D.P. (2002). MicroRNAs in plants. *Genes Dev.* **16**: 1616–1626.
- Riese, M., Höhmann, S., Saedler, H., Münster, T., and Huijser, P. (2007). Comparative analysis of the SBP-box gene families in *P. patens* and seed plants. *Gene* **401**: 28–37.
- Riese, M., Zobell, O., Saedler, H., and Huijser, P. (2008). SBP-domain transcription factors as possible effectors of cryptochrome-mediated blue light signalling in the moss *Physcomitrella patens*. *Planta* **227**: 505–515.
- Rodriguez, R.E., Mecchia, M.A., Debernardi, J.M., Schommer, C., Weigel, D., and Palatnik, J.F. (2010). Control of cell proliferation in *Arabidopsis thaliana* by microRNA miR396. *Development* **137**: 103–112.
- Sambrook, J., Fritsch, E.F., and Maniatis, T. (1989). *Molecular Cloning: A Laboratory Manual*. (Cold Spring Harbor, NY: Cold Spring Harbor Laboratory Press).
- Sanders, P.M., Bui, A.Q., Weterings, K., McIntire, K.N., Hsu, Y.C., Lee, P.Y., Truong, M.T., Beals, T.P., and Goldberg, R.B. (1999). Anther developmental defects in *Arabidopsis thaliana* male-sterile mutants. *Sex. Plant Reprod.* **11**: 297–322.
- Schieffhale, U., Balasubramanian, S., Sieber, P., Chevalier, D., Wisman, E., and Schneitz, K. (1999). Molecular analysis of *NOZZLE*, a gene involved in pattern formation and early sporogenesis during sex organ development in *Arabidopsis thaliana*. *Proc. Natl. Acad. Sci. USA* **96**: 11664–11669.
- Schwab, R., Palatnik, J.F., Riester, M., Schommer, C., Schmid, M., and Weigel, D. (2005). Specific effects of microRNAs on the plant transcriptome. *Dev. Cell* **8**: 517–527.
- Schwarz, S., Grande, A.V., Bujdosó, N., Saedler, H., and Huijser, P. (2008). The microRNA regulated SBP-box genes *SPL9* and *SPL15* control shoot maturation in *Arabidopsis*. *Plant Mol. Biol.* **67**: 183–195.
- Shikata, M., Koyama, T., Mitsuda, N., and Ohme-Takagi, M. (2009). *Arabidopsis* SBP-box genes *SPL10*, *SPL11* and *SPL2* control morphological change in association with shoot maturation in the reproductive phase. *Plant Cell Physiol.* **50**: 2133–2145.
- Smyth, D.R., Bowman, J.L., and Meyerowitz, E.M. (1990). Early flower development in *Arabidopsis*. *Plant Cell* **2**: 755–767.
- Sorensen, A., Guerineau, F., Canales-Holzeis, C., Dickinson, H.G., and Scott, R.J. (2002). A novel extinction screen in *Arabidopsis thaliana* identifies mutant plants defective in early microsporangial development. *Plant J.* **29**: 581–594.
- Sozzani, R., Maggio, C., Giordo, R., Umana, E., Ascencio-Ibañez, J.T., Hanley-Bowdoin, L., Bergounioux, C., Cella, R., and Albani, D. (2010). The E2FD/DEL2 factor is a component of a regulatory network controlling cell proliferation and development in *Arabidopsis*. *Plant Mol. Biol.* **72**: 381–395.
- Stone, J.M., Liang, X., Neel, E.R., and Stiers, J.J. (2005). *Arabidopsis AtSPL14*, a plant-specific SBP-domain transcription factor, participates in plant development and sensitivity to fumonisin B1. *Plant J.* **41**: 744–754.
- Unte, U.S., Sorensen, A.M., Pesaresi, P., Gandikota, M., Leister, D., Saedler, H., and Huijser, P. (2003). *SPL8*, an SBP-box gene that affects pollen sac development in *Arabidopsis*. *Plant Cell* **15**: 1009–1019.
- Usami, T., Horiguchi, G., Yano, S., and Tsukaya, H. (2009). The more and smaller cells mutants of *Arabidopsis thaliana* identify novel roles

- for *SQUAMOSA PROMOTER BINDING PROTEIN-LIKE* genes in the control of heteroblasty. *Development* **136**: 955–964.
- Válóczi, A., Várallyay, E., Kauppinen, S., Burgyán, J., and Havelda, Z.** (2006). Spatio-temporal accumulation of microRNAs is highly coordinated in developing plant tissues. *Plant J.* **47**: 140–151.
- Wang, H., Nussbaum-Wagler, T., Li, B., Zhao, Q., Vigouroux, Y., Faller, M., Bomblies, K., Lukens, L., and Doebley, J.F.** (2005). The origin of the naked grains of maize. *Nature* **436**: 714–719.
- Wang, J.W., Czech, B., and Weigel, D.** (2009). miR156-regulated SPL transcription factors define an endogenous flowering pathway in *Arabidopsis thaliana*. *Cell* **138**: 738–749.
- Wang, J.W., Schwab, R., Czech, B., Mica, E., and Weigel, D.** (2008). Dual effects of miR156-targeted *SPL* genes and *CYP78A5/KLUH* on plastochron length and organ size in *Arabidopsis thaliana*. *Plant Cell* **20**: 1231–1243.
- Wellmer, F., Alves-Ferreira, M., Dubois, A., Riechmann, J.L., and Meyerowitz, E.M.** (2006). Genome-wide analysis of gene expression during early *Arabidopsis* flower development. *PLoS Genet.* **2**: e117.
- Wellmer, F., Riechmann, J.L., Alves-Ferreira, M., and Meyerowitz, E.M.** (2004). Genome-wide analysis of spatial gene expression in *Arabidopsis* flowers. *Plant Cell* **16**: 1314–1326.
- Wijeratne, A.J., Zhang, W., Sun, Y., Liu, W., Albert, R., Zheng, Z., Oppenheimer, D.G., Zhao, D., and Ma, H.** (2007). Differential gene expression in *Arabidopsis* wild-type and mutant anthers: insights into anther cell differentiation and regulatory networks. *Plant J.* **52**: 14–29.
- Wu, G., Park, M.Y., Conway, S.R., Wang, J.W., Weigel, D., and Poethig, R.S.** (2009). The sequential action of miR156 and miR172 regulates developmental timing in *Arabidopsis*. *Cell* **138**: 750–759.
- Wu, G., and Poethig, R.S.** (2006). Temporal regulation of shoot development in *Arabidopsis thaliana* by miR156 and its target *SPL3*. *Development* **133**: 3539–3547.
- Xie, K., Wu, C., and Xiong, L.** (2006). Genomic organization, differential expression, and interaction of *SQUAMOSA* promoter-binding-like transcription factors and microRNA156 in rice. *Plant Physiol.* **142**: 280–293.
- Xing, S., Rosso, M.G., and Zachgo, S.** (2005). *ROXY1*, a member of the plant glutaredoxin family, is required for petal development in *Arabidopsis thaliana*. *Development* **132**: 1555–1565.
- Xing, S., and Zachgo, S.** (2008). *ROXY1* and *ROXY2*, two *Arabidopsis* glutaredoxin genes, are required for anther development. *Plant J.* **53**: 790–801.
- Yamasaki, H., Hayashi, M., Fukazawa, M., Kobayashi, Y., and Shikanai, T.** (2009). *SQUAMOSA* Promoter Binding Protein-Like7 is a central regulator for copper homeostasis in *Arabidopsis*. *Plant Cell* **21**: 347–361.
- Yamasaki, K., et al.** (2004). A novel zinc-binding motif revealed by solution structures of DNA-binding domains of Arabidopsis SBP-family transcription factors. *J. Mol. Biol.* **337**: 49–63.
- Yang, H.P., Schmuke, J.J., Flagg, L.M., Roberts, J.K., Allen, E.M., Ivashuta, S., Gilbertson, L.A., Armstrong, T.A., and Christian, A.T.** (2009). A novel real-time polymerase chain reaction method for high throughput quantification of small regulatory RNAs. *Plant Biotechnol. J.* **7**: 621–630.
- Yang, S.L., Xie, L.F., Mao, H.Z., Pua, C.S., Yang, W.C., Jiang, L., Sundaresan, V., and Ye, D.** (2003). *Tapetum determinant1* is required for cell specialization in the *Arabidopsis* anther. *Plant Cell* **15**: 2792–2804.
- Yang, W.C., Ye, D., Xu, J., and Sundaresan, V.** (1999). The *SPORO-CYTELESS* gene of *Arabidopsis* is required for initiation of sporogenesis and encodes a novel nuclear protein. *Genes Dev.* **13**: 2108–2117.
- Yu, N., Cai, W.J., Wang, S., Shan, C.M., Wang, L.J., and Chen, X.Y.** (2010). Temporal control of trichome distribution by microRNA156-targeted *SPL* genes in *Arabidopsis thaliana*. *Plant Cell* **22**: 2322–2335.
- Zhang, Y.** (2005). The SBP-Box Gene *SPL8* Affects Reproductive Development and Gibberellin Response in *Arabidopsis*. PhD dissertation (Cologne, Germany: University of Cologne).
- Zhang, Y., Schwarz, S., Saedler, H., and Huijser, P.** (2007). *SPL8*, a local regulator in a subset of gibberellin-mediated developmental processes in *Arabidopsis*. *Plant Mol. Biol.* **63**: 429–439.
- Zhao, D.** (2009). Control of anther cell differentiation: A teamwork of receptor-like kinases. *Sex. Plant Reprod.* **22**: 221–228.
- Zhao, D.Z., Wang, G.F., Speal, B., and Ma, H.** (2002). The excess *microsporocytes1* gene encodes a putative leucine-rich repeat receptor protein kinase that controls somatic and reproductive cell fates in the *Arabidopsis* anther. *Genes Dev.* **16**: 2021–2031.
- Zik, M., and Irish, V.F.** (2003). Global identification of target genes regulated by *APETALA3* and *PISTILLATA* floral homeotic gene action. *Plant Cell* **15**: 207–222.